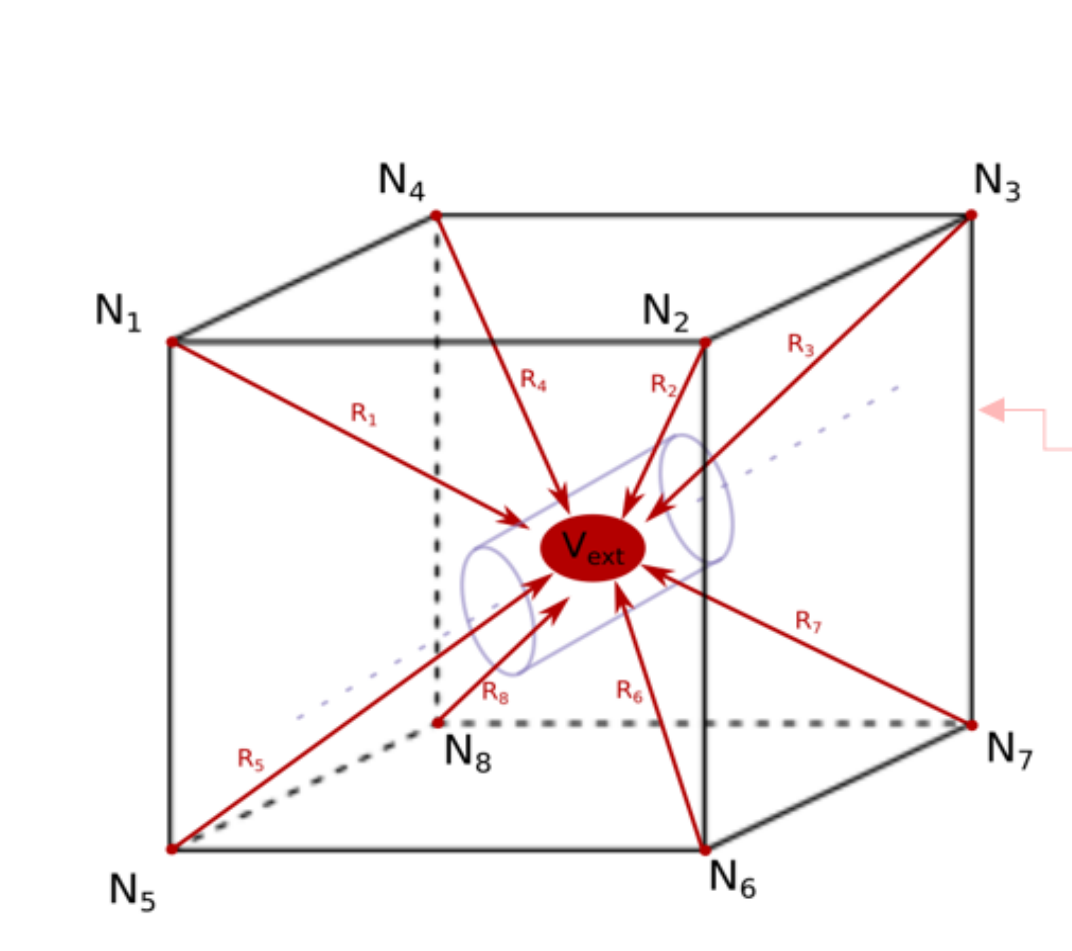
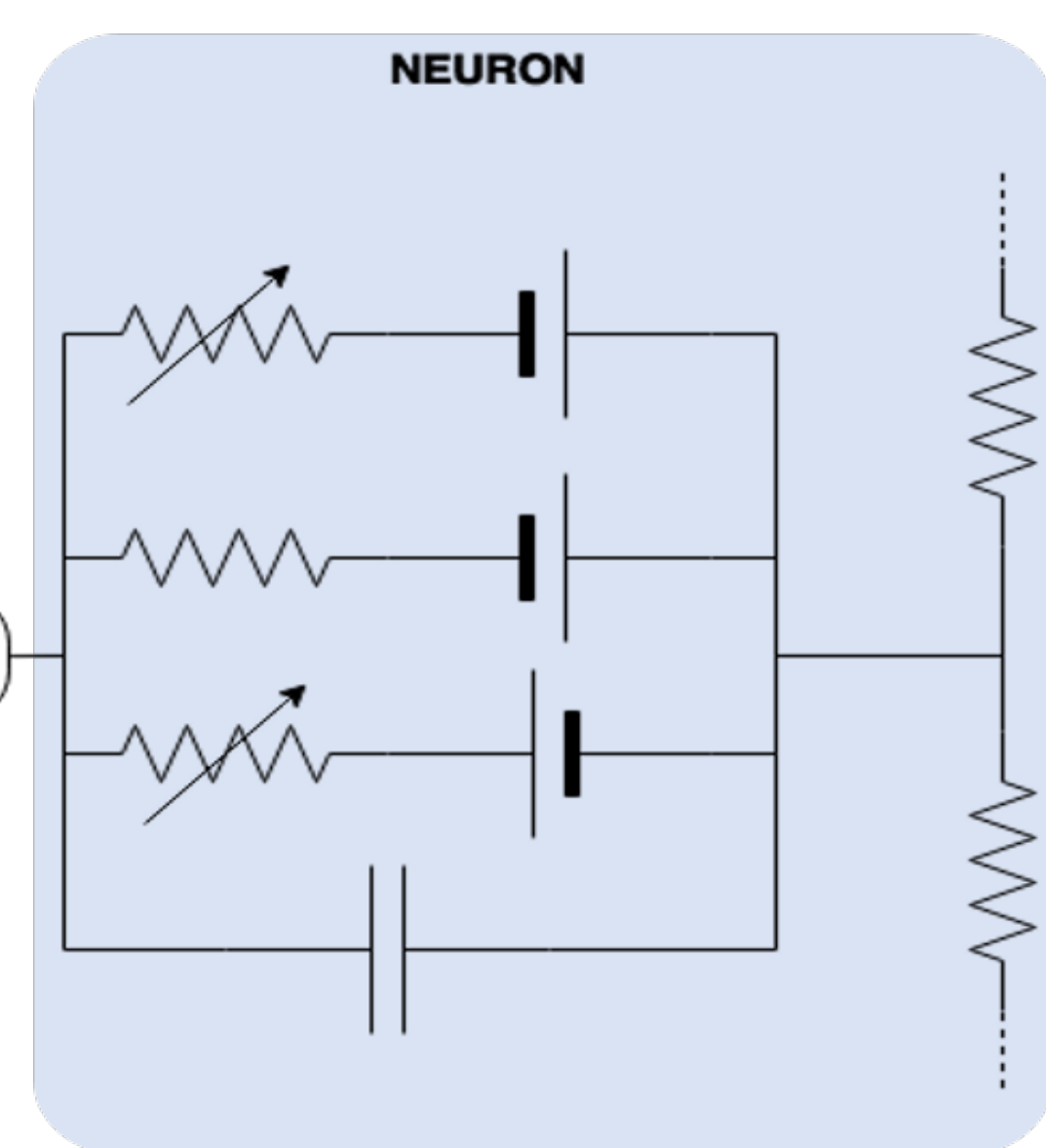
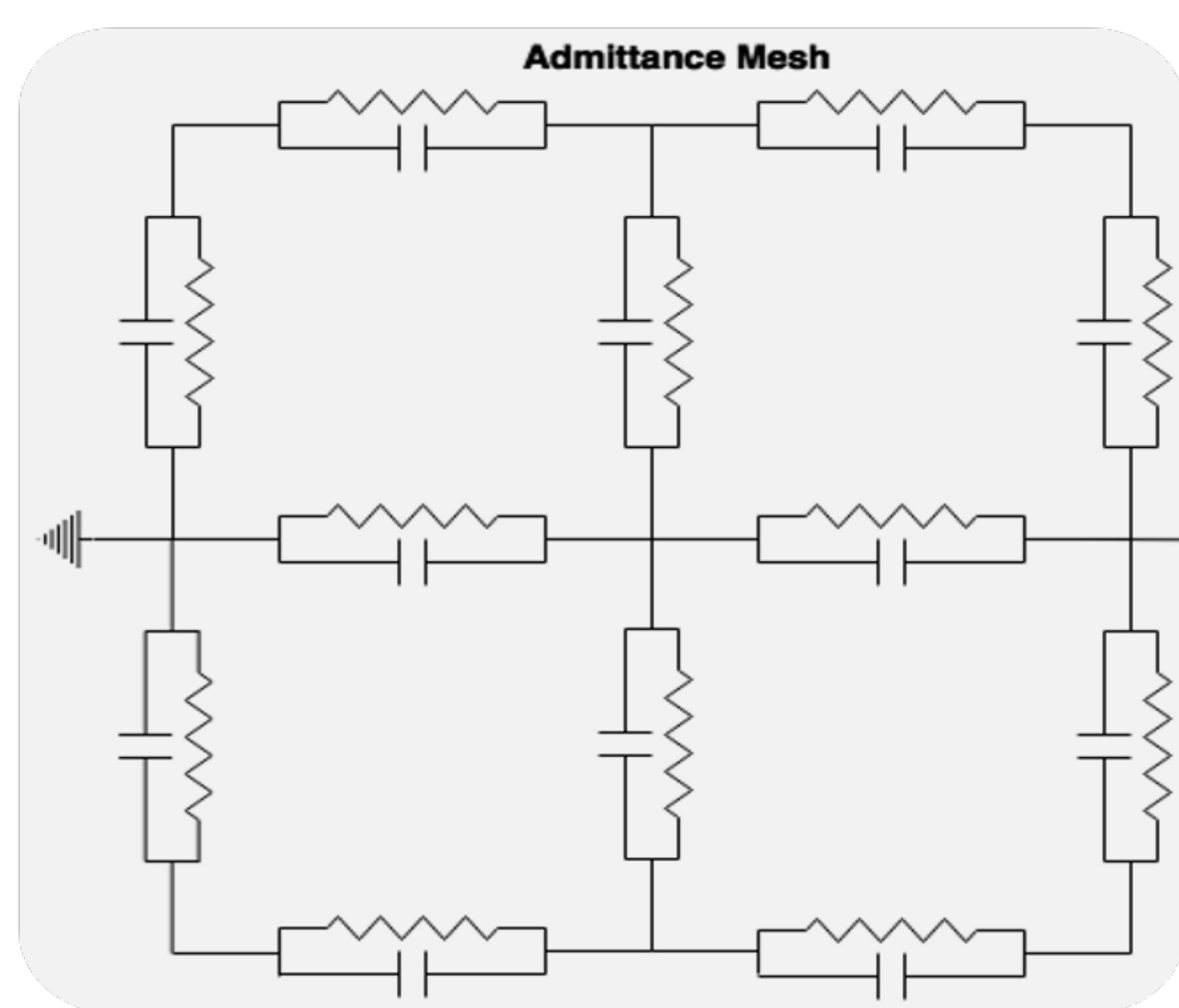


Introduction

The ideal form of a neural-interfacing device is highly dependent upon the anatomy of the region with which it is meant to interface. Multiple-electrode arrays provide a system which can be adapted to various neural geometries. Computational models of stimulating systems have proven useful for evaluating electrode placement and stimulation protocols, but have yet to be adequately adapted to the unique features of the hippocampus.

As an approach to understanding potential memory restorative devices, an Admittance Method-NEURON model was constructed to predict the direct and synaptic response of a 400 micron-thick region of the rat dentate gyrus to electrical stimulation of the perforant path. The volume contained 50,000 unique granule cells and 10,000 explicitly modeled entorhinal cortical axons, making up over 11 million simultaneously solved compartments. These two layers were connected by 11.625 million synapses.

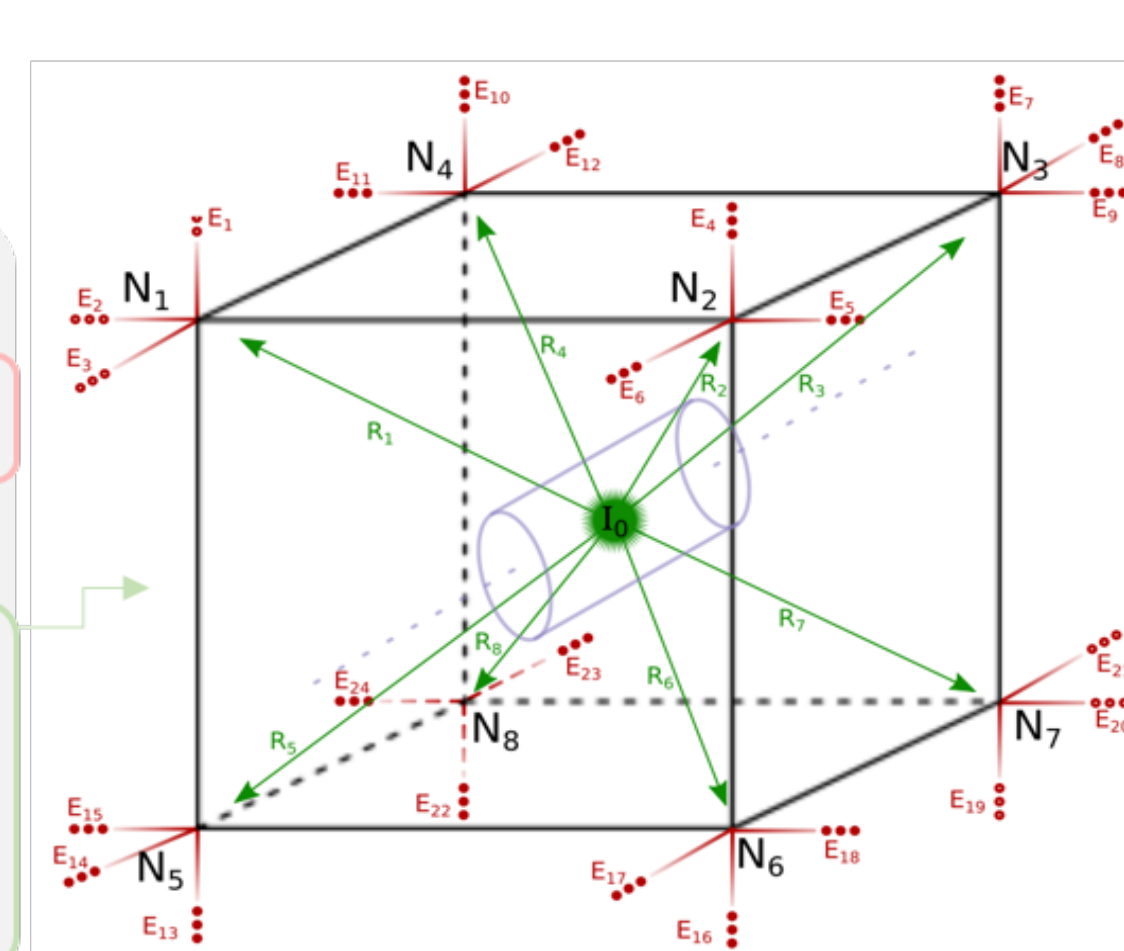
Methods



```

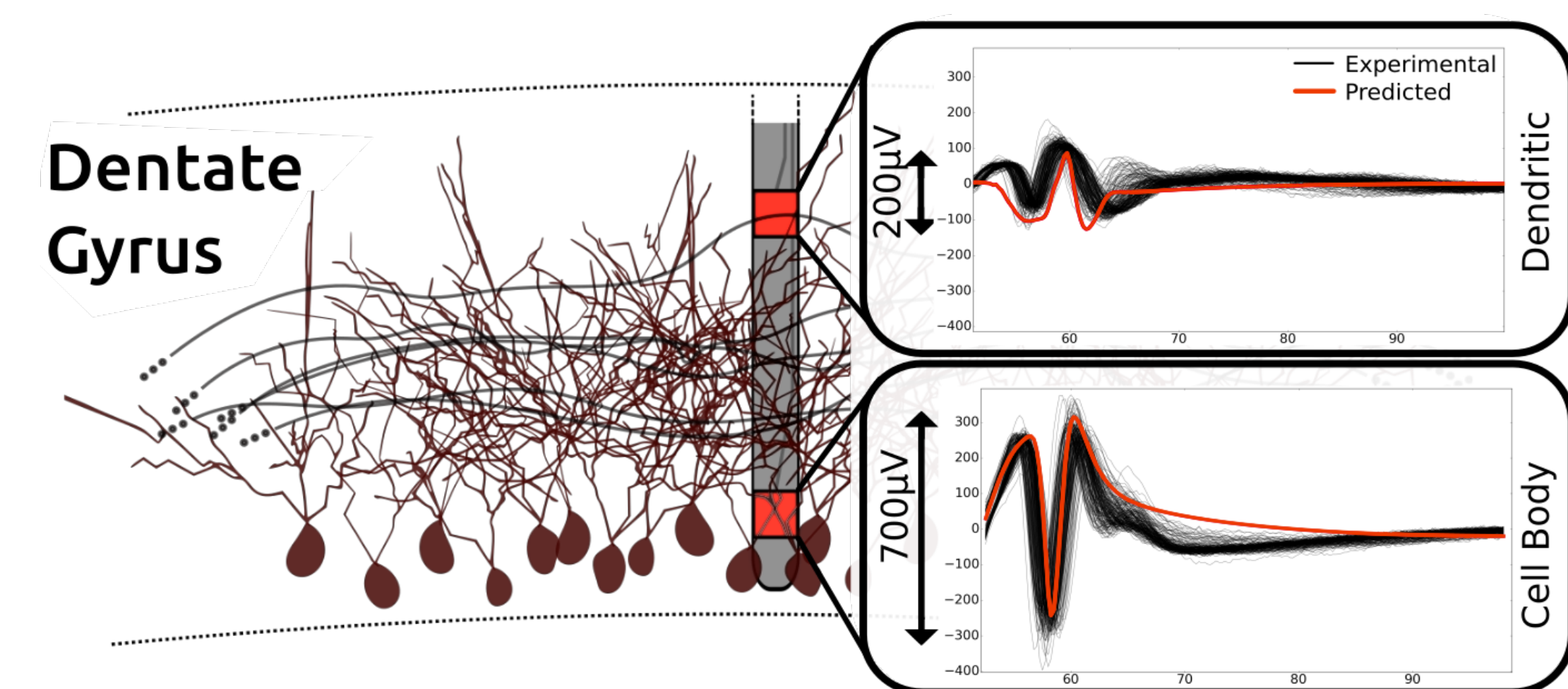
1 For t in simulated_time:
2   Solve AM nodal voltages at time == t
3   For each compartment in NEURON.compartments:
4     compartment.extracellular_voltage = distance-weighted ave. of 8 nearest node voltages
5
6   Solve NEURON at time == t
7   For each compartment in NEURON.compartments:
8     calculate compartmental membrane current density
9   For each node in eight nearest AM nodes:
10    node.current = distance-weighted fraction of compartment current density
11  For each edge in 3 node edges leading away from compartment source:
12    edge.current = resistance-weighted fraction of node.current
13
14 end process

```



Co-simulating model representations of both intracellular and extracellular space can be used to approximate complex neural network responses to extracellular potentials.

Results



Predicted LFPs (red signal) exhibit a characteristic population spike (PS) as observed in experimental evoked potentials (black signals) elicited by a 200 μA biphasic, square-wave pulse [3].

Spiking activity at most locations saturates above stimulus amplitudes of ~500 μA (shown at right). (A) When stimulating at cell body locations, granule cell activity versus stimulus amplitude follows a sigmoidal trend. (B) When stimulating at PP locations, the trend is more logarithmic. (C) The differences between (A) and (B) gives rise to greater efficiency at low amplitude when stimulating in the PP.

For nearly all stimulating conditions the half-height width (HHW) of PS was shorter (ms) when stimulating at the cell body layer and PP at the crest relative to the supra and infrapyramidal transverse locations (D, above). While more variable, nearly all stimulating amplitudes resulted in larger peak PS amplitudes (%) at the crest relative to supra/infra locations.

$$U = \frac{w_1 PS_{max} + w_2 PS_{efficiency} + w_3 [max(HHW) - HHW]}{w_1 + w_2 + w_3}$$

Output of the multi-objective optimization function (U, above) for MPP/LPP (E, left) and CBL (E, right) stimulation cases is presented in the panel to the right. High values of U indicate strong PS. The PS amplitude and power efficiency were maximized and the half-height width was minimized with equal weighting in this optimization. (CBL-cell body layer, MPP/LPP-medial/lateral perforant path).

Conclusions

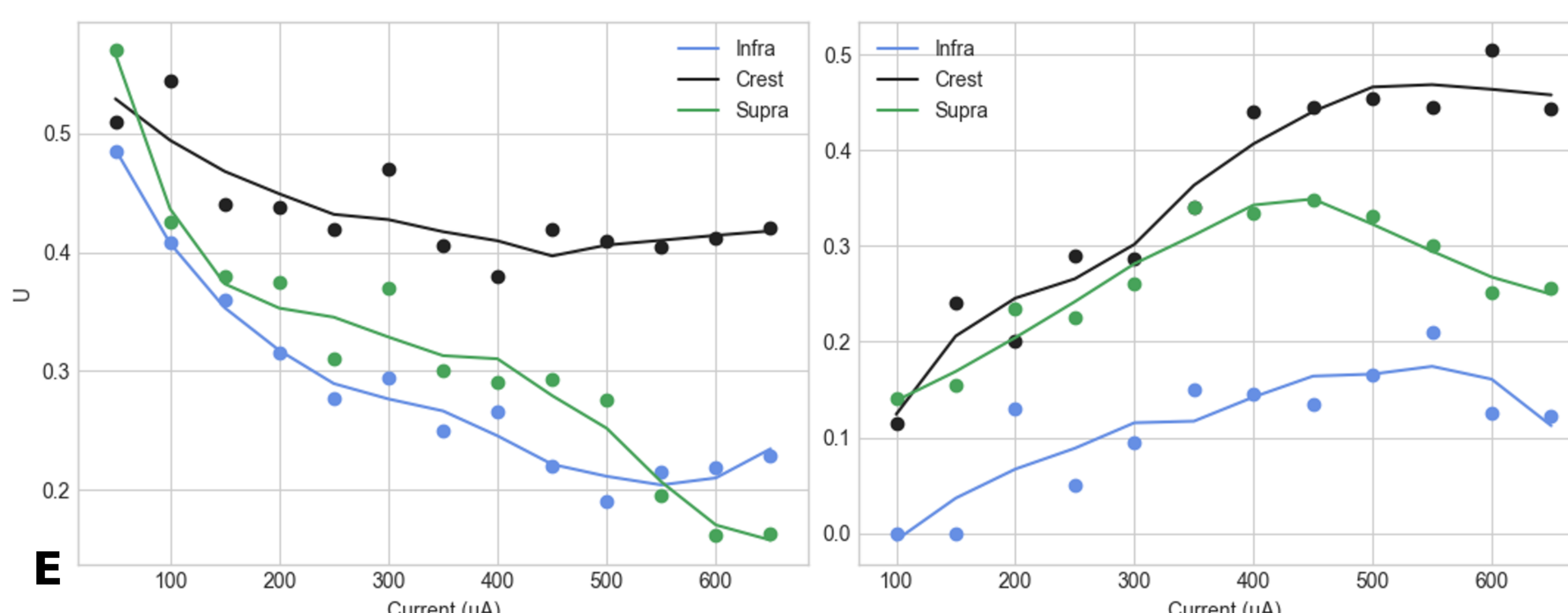
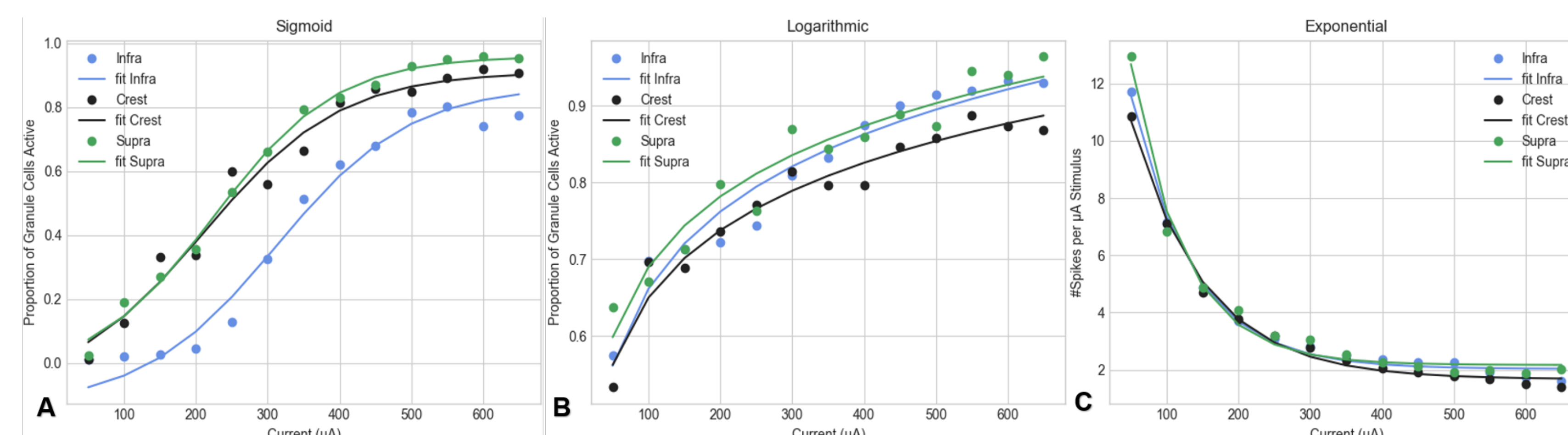
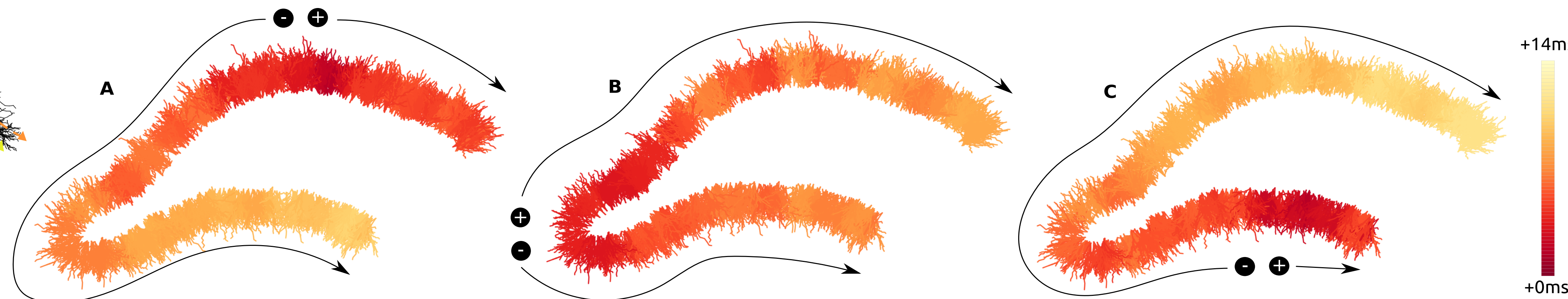
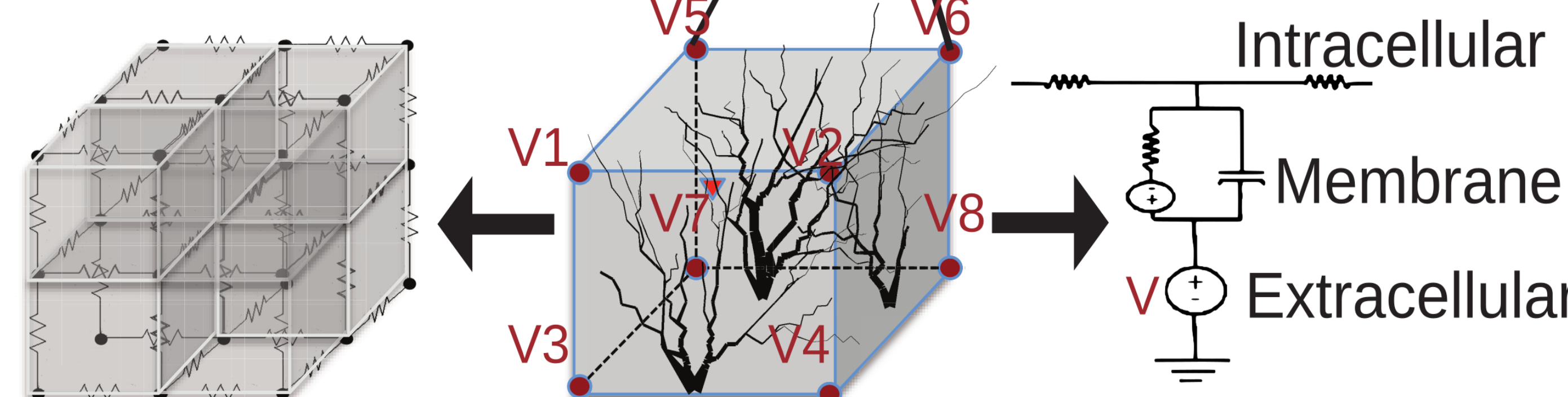
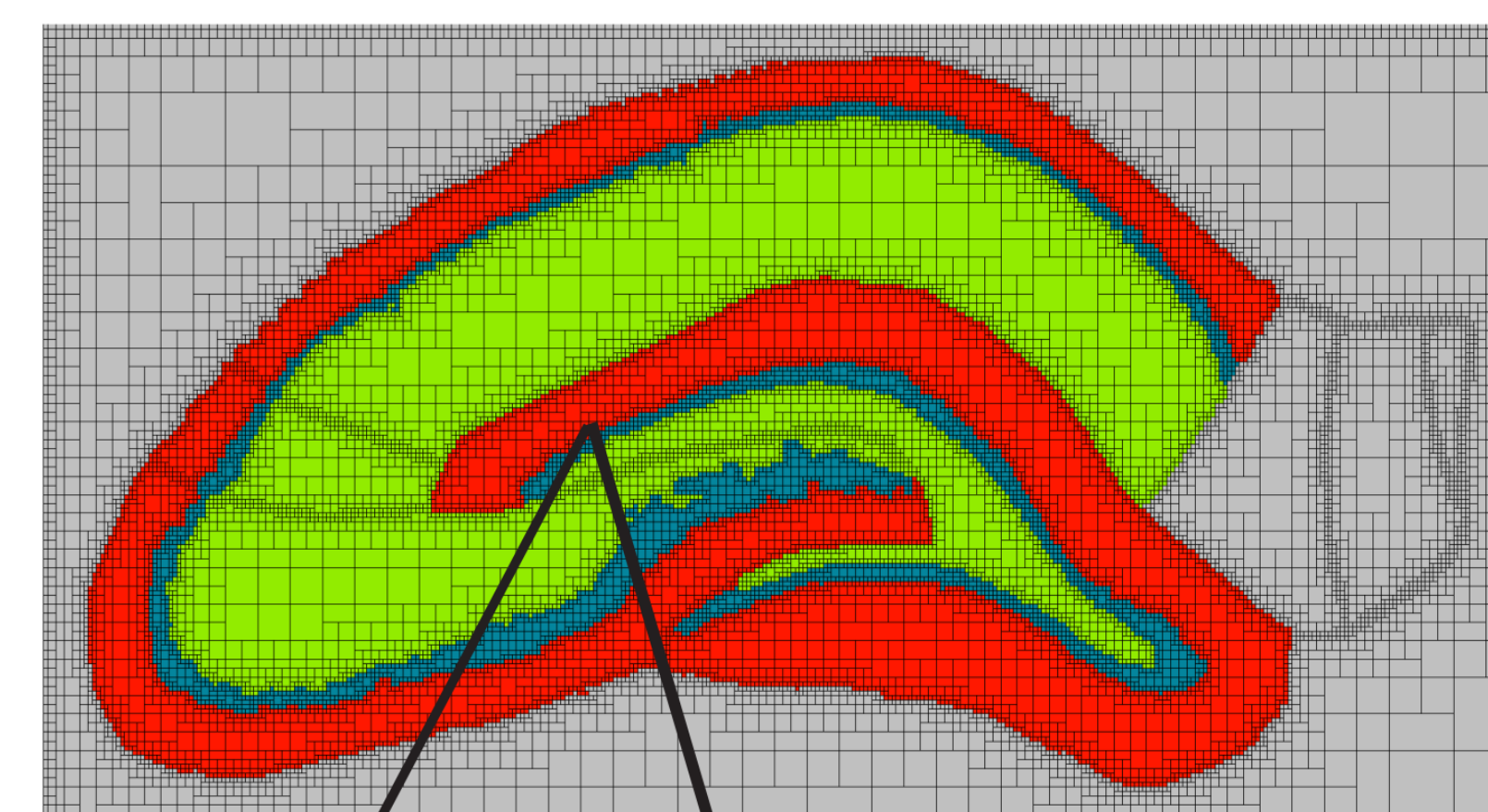
This study presents a model that performs the minimum functions necessary to improve electrical stimulation systems. As the detailed neuronal componentry of the model is further expanded to include more cell types and layers of tissue it will provide a deeper understanding of both the network properties of the hippocampal circuit and better strategies of inducing and recording activity via arrays of electrodes.

Acknowledgements

Research supported by U.S. NIH Grant 1U01GM104604. Computation was supported by the University of Southern California Center for High-Performance Computing and Communications.

Resistivity (Ohm-m)

- 3.212
- 2.879
- 2.605
- 6.429



References

1. T.W. Berger et al. (2011). A cortical neural prosthesis for restoring and enhancing memory. - J Neural Eng Aug;8(4):046017
2. Grill Jr, W. M. (1999). Modeling the effects of electric fields on nerve fibers: influence of tissue electrical properties. Biomedical Engineering, IEEE Transactions on, 46 (8), 918-928.
3. W., Soussou et al. (2006). Mapping Spatio-Temporal Electrophysiological Activity in Hippocampal Slices with Conformal Planar Multi-Electrode Arrays. Advances in Network Electrophysiology - Using Multi-Electrode Arrays, (4), 127-152.
4. Hines, M. L., & Carnevale, N. T. (1997). The NEURON simulation environment. Neural Computation, 9(6), 1179-1209. <http://doi.org/10.1162/neco.1997.9.6.1179>
5. C.S., Bingham et al. (2018). Model-Based Analysis of Electrode Placement and Pulse Amplitude for Hippocampal Stimulation. IEEE Trans. Biomed. Eng. doi:10.1109/TBME.2018.2791860
6. C.S., Bingham et al. (2016). A large-scale detailed neuronal model of electrical stimulation of the dentate gyrus and perforant path as a platform for electrode design and optimization. In 2016 38th Annual International Conference of the IEEE Engineering in Medicine and Biology Society (EMBC) (pp. 2794-2797). IEEE.